

## ISL6219A

Microprocessor CORE Voltage Regulator Precision Multi-Phase BUCK PWM Controller for Mobile Applications

FN9093  
Rev.1.00  
Mar 20, 2007

The ISL6219A provides core-voltage regulation by driving up to three interleaved synchronous-rectified buck-converter channels in parallel. Intersil multi-phase controllers together with ISL6207 gate drivers form the basis for the most reliable power-supply solutions available to power the latest industry-leading microprocessors. Multi-phase buck-converter architecture uses interleaved timing to multiply ripple frequency and reduce input and output ripple currents. Lower ripple results in lower total component cost, reduced dissipation, and smaller implementation area. Pre-configured for 3-phase operation, the ISL6219A offers the flexibility of 2-phase operation. Simply connect the unused PWM pin to +5V. The channel switching frequency is adjustable in the range of 100kHz to 1.5MHz giving the designer the ultimate flexibility in managing the balance between high-speed response and good thermal management.

New features on the ISL6219A include Dynamic-VID™ technology allowing seamless on-the-fly VID changes with no need for any additional external components. When the ISL6219A receives a new VID code, it incrementally steps the output voltage to the new level. Dynamic VID™ changes are fast and reliable with no output voltage overshoot or undershoot.

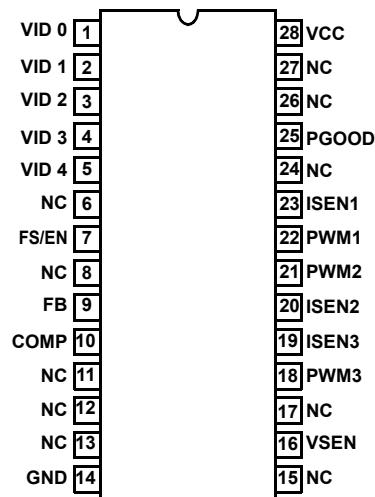
Like other Intersil multiphase controllers, the ISL6219A uses cost and space-saving  $r_{DS(ON)}$  sensing for channel current balance and dynamic voltage positioning. Channel current balancing is automatic and accurate with the integrated current-balance control system. Overcurrent protection can be tailored to any application with no need of additional parts.

An integrated DAC decodes the 5-bit logic signal present at VID0-VID4 and provides an accurate reference for precision voltage regulation. The high-bandwidth error amplifier and accurate voltage reference all work together to provide better than 0.8% total system accuracy, and to enable the fastest transient response available. A window comparator toggles PGOOD if the output voltage moves out of range and acts to protect the load in case of overvoltage.

### Features

- Multi-Phase Power Conversion
- Active Channel Current Balancing
- Lossless current sense scheme
  - Uses MOSFET's  $r_{DS(ON)}$
  - Optional current sense method for higher precision
- Precision CORE Voltage Regulation
  - $\pm 0.8\%$  System Accuracy Over Temperature
- Microprocessor Voltage Identification Input
  - Dynamic VID technology
  - 5-Bit VID Input
  - 1.100V to 1.850V in 25mV Steps
- Programmable Droop Voltage
- Fast Transient Recovery Time
- Overvoltage, Undervoltage and Overcurrent Protection
- Power-Good Output
- 2 or 3 Phase Operation
- User selectable Switching Frequency of 100kHz to 1.5MHz
  - 200kHz - 4.5MHz Effective Ripple Frequency

ISL6219A  
(28 LD QSOP)  
TOP VIEW



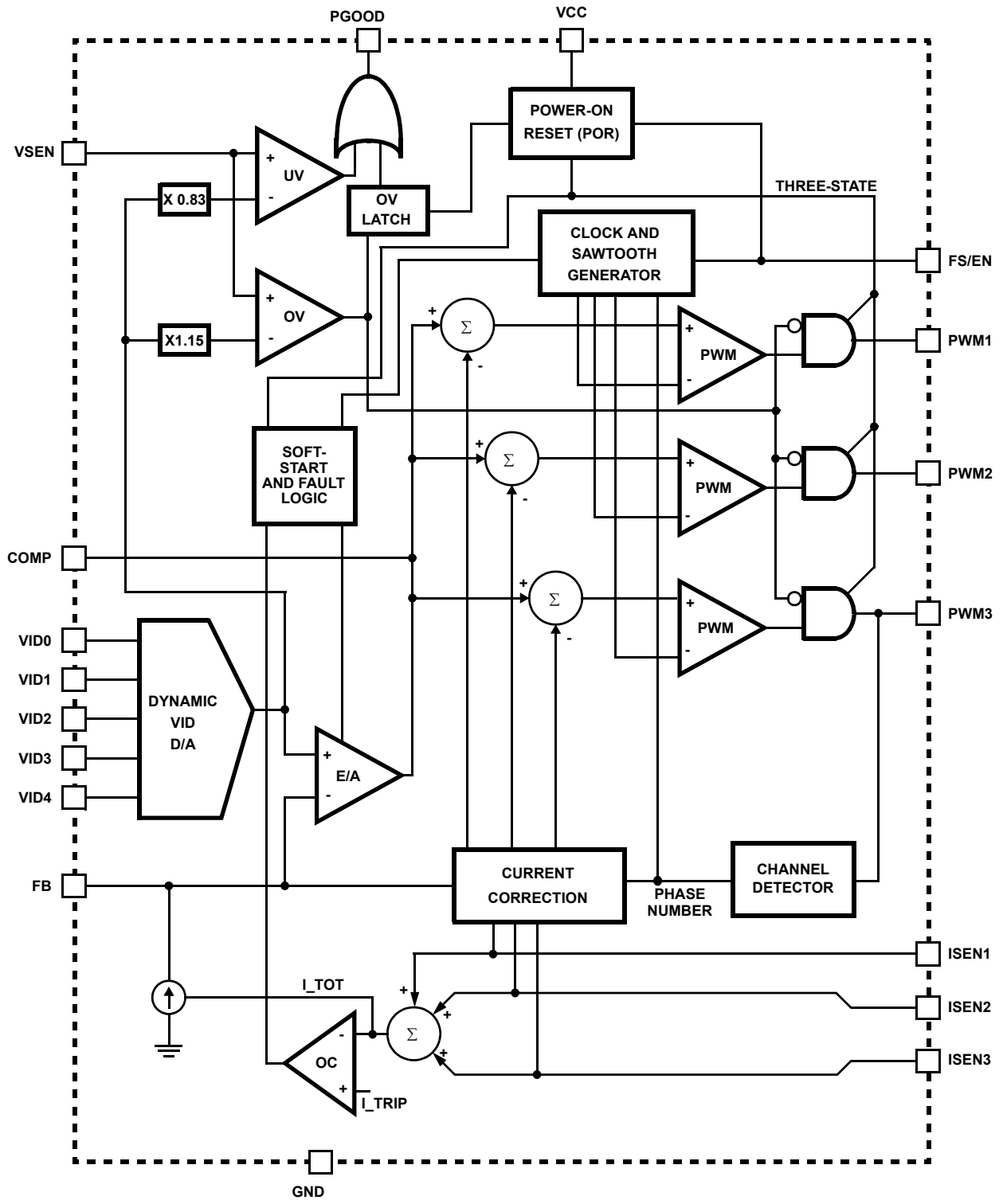
### Ordering Information

PART NUMBER	PART MARKING	TEMP. RANGE (°C)	PACKAGE	PKG. DWG. #
ISL6219ACA*	ISL 6219ACA	-10 to +85	28 Ld QSOP	M28.15
ISL6219ACAZ* (Note)	ISL6219 ACAZ	-10 to +85	28 Ld QSOP (Pb-free)	M28.15

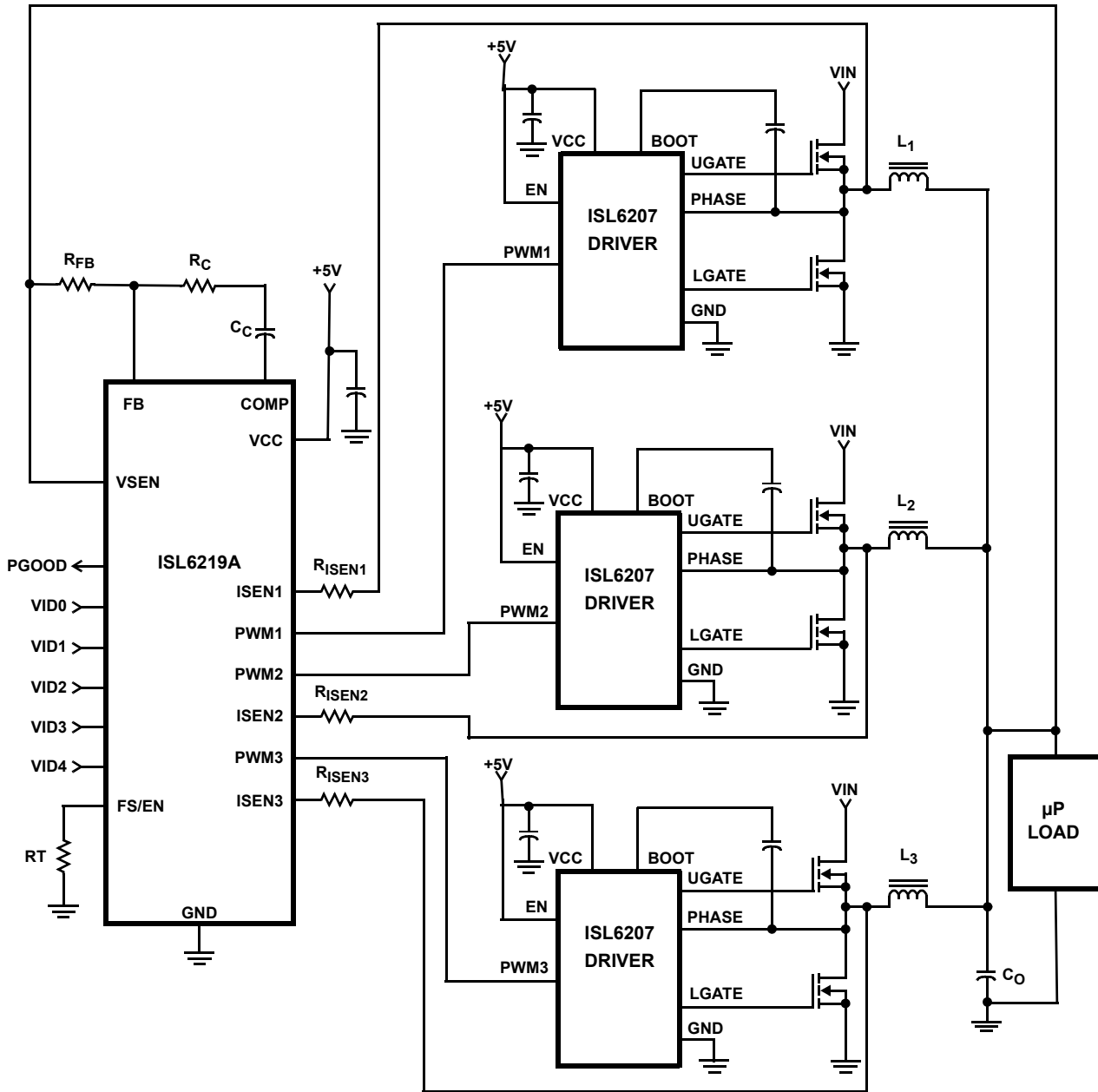
\*Add "-T" suffix for tape and reel.

NOTE: Intersil Pb-free plus anneal products employ special Pb-free material sets; molding compounds/die attach materials and 100% matte tin plate termination finish, which are RoHS compliant and compatible with both SnPb and Pb-free soldering operations. Intersil Pb-free products are MSL classified at Pb-free peak reflow temperatures that meet or exceed the Pb-free requirements of IPC/JEDEC J STD-020.

**Block Diagram**



**Typical Application - 3-Phase Buck Converter**



**Absolute Maximum Ratings**

Supply Voltage, VCC . . . . . 7V  
 Input, Output, or I/O Voltage . . . . . GND -0.3V to V<sub>CC</sub> + 0.3V  
 ESD Classification . . . . . 3kV

**Recommended Operating Conditions**

Supply Voltage . . . . . +5V ±5%  
 Ambient Temperature . . . . . -10°C to +85°C

**Thermal Information**

Thermal Resistance (Typical, Note 1)  $\theta_{JA}$  (°C/W)  
 SSOP Package (Note 1) . . . . . 76  
 Maximum Junction Temperature . . . . . +150°C  
 Maximum Storage Temperature Range . . . . . -65°C to +150°C  
 Maximum Lead Temperature (Soldering 10s) . . . . . +300°C  
 (SSOP - Lead Tips Only)

*CAUTION: Stress above those listed in "Absolute Maximum Ratings" may cause permanent damage to the device. This is a stress only rating and operation of the device at these or any other conditions above those indicated in the operational section of this specification is not implied.*

*+150°C max junction temperature is intended for short periods of time to prevent shortening the lifetime. Operation close to +150°C junction may trigger the shutdown of the device even before +150°C, since this number is specified as typical.*

**NOTE:**

1.  $\theta_{JA}$  is measured with the component mounted on a high effective thermal conductivity test board in free air. (See Tech Brief TB379 for details.)

Electrical Specifications      Operating Conditions: V<sub>CC</sub> = 5V, T<sub>A</sub> = -10°C to +85°C, Unless Otherwise Specified

PARAMETER	TEST CONDITIONS	MIN	TYP	MAX	UNITS
<b>INPUT SUPPLY POWER</b>					
Input Supply Current	RT = 100k $\Omega$ , FS/EN = 1.23V	-	9.3	15	mA
	RT = 100k $\Omega$ , FS/EN = 0V	4.5	8.8	14	mA
Power-On Reset Threshold	VCC Rising	4.25	4.38	4.5	V
	VCC Falling	3.75	3.88	4.0	V
<b>SYSTEM ACCURACY</b>					
System Accuracy		-0.8	-	0.8	%VID
VID Pull Up		-	2.5	-	V
VID Input Low Level		-	-	0.8	V
VID Input High Level (Note 3)		2.0	-	-	V
<b>OSCILLATOR</b>					
Accuracy		-20	-	20	%
Frequency	RT = 100k $\Omega$ ( $\pm 1\%$ )	224	280	336	kHz
Adjustment Range	Guaranteed by characterization	100		1500	kHz
Disable Voltage		-	1.23	1.1	V
Sawtooth Amplitude		-	1.54	-	V
Duty-Cycle Range Functional		0	-	75	%
<b>ERROR AMPLIFIER</b>					
Open-Loop Gain		-	72	-	dB
Open-Loop Bandwidth		-	18	-	MHz
Slew Rate	CL = 100pF, RL = 10k $\Omega$ to ground	-	5.3	-	V/ $\mu$ s
Maximum Output Voltage	RL = 10k $\Omega$ to ground	3.6	4.1	-	V
Minimum Output Voltage	RL = 10k $\Omega$ to ground	-	0.23	0.5	V
<b>I<sub>SEN</sub></b>					
Full Scale Input Current		-	50	-	$\mu$ A
Overcurrent Trip Level		-	75	-	$\mu$ A
<b>POWER GOOD MONITOR</b>					
PGOOD Low Output Voltage	I <sub>PGOOD</sub> = 4mA	-	0.18	0.4	V

PARAMETER	TEST CONDITIONS	MIN	TYP	MAX	UNITS
<b>PROTECTION and MONITOR</b>					
Overvoltage Threshold	VSEN Rising	112	115	12	%V <sub>DAC</sub>
	VSEN Falling	-	VID	-	%V <sub>DAC</sub>
Undervoltage Threshold	VSEN Rising	85	92	95	%V <sub>DAC</sub>
	VSEN Falling	80	83	90	%V <sub>DAC</sub>

NOTES:

2. These parts are designed and adjusted for accuracy within the system tolerance given in the Electrical Specifications. The system tolerance accounts for offsets in the differential and error amplifiers; reference-voltage inaccuracies; temperature drift; and the full DAC adjustment range.
3. VID input levels above 2.9V may produce an reference-voltage offset inaccuracy. Use a current limit resistor when pull up to 5V.

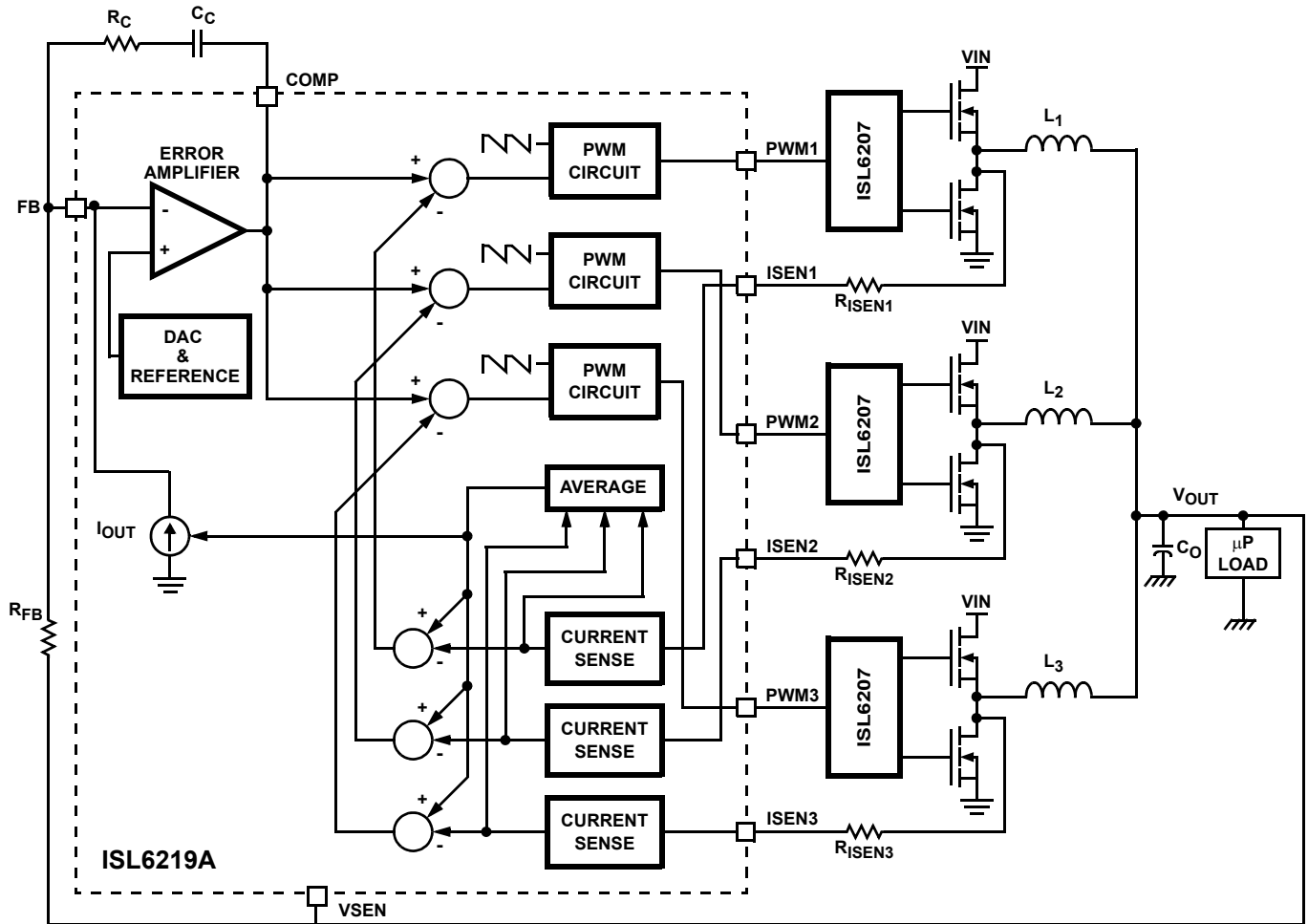


FIGURE 1. SIMPLIFIED BLOCK DIAGRAM OF THE ISL6219A

## Operation

### Multi-Phase Power Conversion

Multi-phase power conversion provides the most cost-effective power solution when load currents are no longer easily supported by single-phase converters. Although its greater complexity presents additional technical challenges, the multi-phase approach offers cost-saving advantages with improved response time, superior ripple cancellation, and excellent thermal distribution.

### INTERLEAVING

The switching of each channel in a multi-phase converter is timed to be symmetrically out of phase with each of the other channels. In a 3-phase converter, each channel switches 1/3 cycle after the previous channel and 1/3 cycle before the following channel. As a result, the three-phase converter has a combined ripple frequency three times greater than the ripple frequency of any one phase. In addition, the peak-to-peak amplitude of the combined inductor currents is reduced in proportion to the number of phases (Equations 1 and 2). Increased ripple frequency and lower ripple amplitude mean that the designer can use less per-channel inductance and lower total output capacitance for any performance specification.

Figure 2 illustrates the multiplicative effect on output ripple frequency. The three channel currents (IL1, IL2, and IL3), combine to form the AC ripple current and the DC load current. The ripple component has three times the ripple frequency of each individual channel current. Each PWM pulse is terminated 1/3 of a cycle after the PWM pulse of the previous phase. The peak-to-peak current waveforms for each phase is about 7A, and the dc components of the inductor currents combine to feed the load.

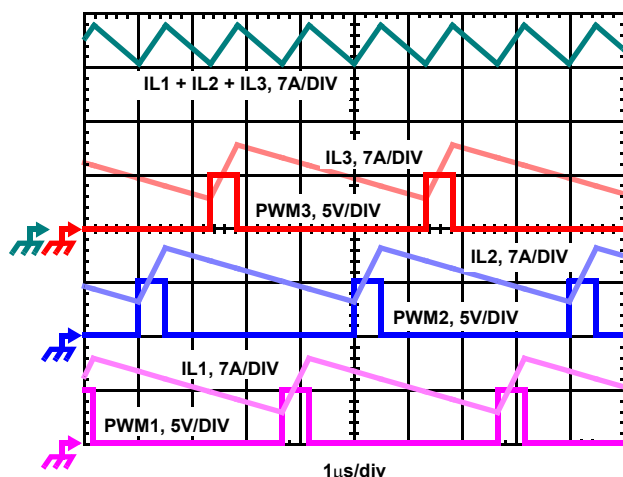


FIGURE 2. PWM AND INDUCTOR-CURRENT WAVEFORMS FOR 3-PHASE CONVERTER

To understand the reduction of ripple current amplitude in the multi-phase circuit, examine the equation representing an individual channel's peak-to-peak inductor current.

$$I_{L,PP} = \frac{(V_{IN} - V_{OUT})V_{OUT}}{L f_S V_{IN}} \quad (\text{EQ. 1})$$

In Equation 1,  $V_{IN}$  and  $V_{OUT}$  are the input and output voltages respectively,  $L$  is the single-channel inductor value, and  $f_S$  is the switching frequency.

$$I_{PP} = \frac{(V_{IN} - N V_{OUT})V_{OUT}}{L f_S V_{IN}} \quad (\text{EQ. 2})$$

The output capacitors conduct the ripple component of the inductor current. In the case of multi-phase converters, the capacitor current is the sum of the ripple currents from each of the individual channels. Compare Equation 1 to the expression for the peak-to-peak current after the summation of  $N$  symmetrically phase-shifted inductor currents in Equation 2. Peak-to-peak ripple current decreases by an amount proportional to the number of channels. Output voltage ripple is a function of capacitance, capacitor equivalent series resistance (ESR), and inductor ripple current. Reducing the inductor ripple current allows the designer to use fewer or less costly output capacitors.

Another benefit of interleaving is to reduce input ripple current. Input capacitance is determined in part by the maximum input ripple current. Multi-phase topologies can improve overall system cost and size by lowering input ripple current and allowing the designer to reduce the cost of input capacitance. The example in Figure 3 illustrates input currents from a three-phase converter combining to reduce the total input ripple current.

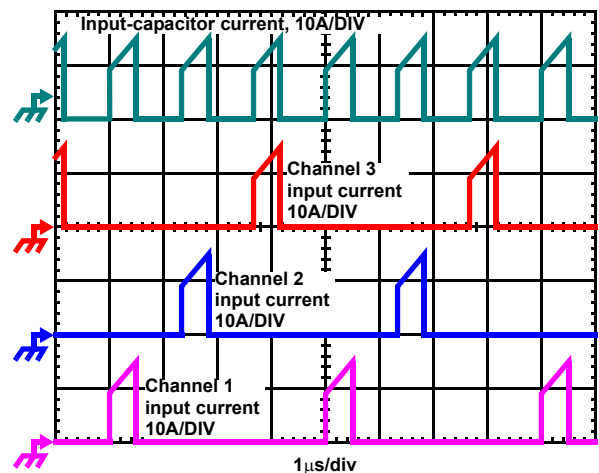


FIGURE 3. CHANNEL INPUT CURRENTS AND INPUT-CAPACITOR RMS CURRENT FOR 3-PHASE

The converter depicted in Figure 3 delivers 36A to a 1.5V load from a 12V input. The RMS input capacitor current is 5.9A. Compare this to a single-phase converter also down 12V to 1.5V at 36A. The single-phase converter has 11.9A rms input capacitor current. The single-phase converter must use an input capacitor bank with twice the RMS current capacity as the equivalent three-phase converter.

Figures 14 and 15 in the section entitled <italic> can be used to determine the input-capacitor rms current based on load current, duty cycle, and the number of active channels. They are provided as aids in determining the optimal input capacitor solution. Figure 16 shows the single phase input-capacitor rms current for comparison.

## PWM OPERATION

The number of active channels selected determines the timing for each channel. By default, the timing mode for the ISL6219A is 3-phase. The designer can select 2-phase timing by connecting PWM3 to VCC.

One switching cycle for the ISL6219A is defined as the time between PWM1 pulse termination signals (the internal signal that initiates a falling edge on PWM1). The cycle time is the inverse of the switching frequency selected by the resistor connected between the FS/EN pin and ground (see <italic>Switching Frequency). Each cycle begins when a clock signal commands the channel-1 PWM output to go low. This signals the channel-1 MOSFET driver to turn off the channel-1 upper MOSFET and turn on the channel-1 synchronous MOSFET. If two-channel operation is selected, the PWM2 pulse terminates 1/2 of a cycle later. If three channels are selected the PWM2 pulse terminates 1/3 of a cycle after PWM1, and the PWM3 output will follow after another 1/3 of a cycle.

Once a channel's PWM pulse terminates, it remains low for a minimum of 1/4 cycle. This forced off time is required to assure an accurate current sample as described in <italic>Current Sensing. Following the 1/4-cycle forced off time, the controller enables the PWM output. Once enabled, the PWM output transitions high when the sawtooth signal crosses the adjusted error-amplifier output signal,  $V_{COMP}$  as illustrated in Figures 1 and 5. This is the signal for the MOSFET driver to turn off the synchronous MOSFET and turn on the upper MOSFET. The output will remain high until the clock signals the beginning of the next cycle by commanding the PWM pulse to terminate.

## CURRENT SENSING

Intersil multi-phase controllers sense current by sampling the voltage across the lower MOSFET during its conduction interval. MOSFET  $r_{DS(ON)}$  sensing is a no-added-cost method to sense current for load-line regulation, channel-current balance, module current sharing, and overcurrent protection. If desired, an independent current-sense resistor in series with the lower-MOSFET source can serve as a sense element in place of the MOSFET  $r_{DS(ON)}$ .

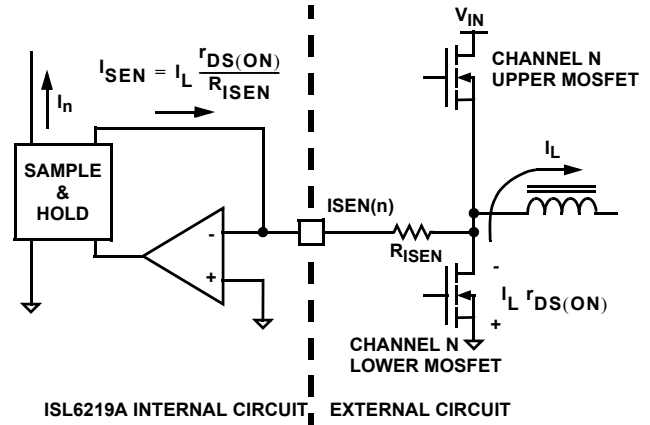


FIGURE 4. INTERNAL AND EXTERNAL CURRENT-SENSING CIRCUITRY

The ISEN input for each channel uses a ground-referenced amplifier to reproduce a signal proportional to the channel current (Figure 4). After sufficient settling time, the sensed current is sampled, and the sample is used for current balance, load-line regulation and overcurrent protection. The ISL6219A samples channel current once each cycle. Figure 4 shows how the sampled current,  $I_n$ , is created from the channel current  $I_L$ . The circuitry in Figure 4 represents the current measurement and sampling circuitry for channel n in an N-channel converter. This circuitry is repeated for each channel in the converter but will not be active in unused channels.

## CHANNEL-CURRENT BALANCE

Another benefit of multi-phase operation is the thermal advantage gained by distributing the dissipated heat over multiple devices and greater area. By doing this, the designer avoids the complexity of driving multiple parallel MOSFETs and the expense of using expensive heat sinks and exotic magnetic materials.

In order to fully realize the thermal advantage, it is important that each channel in a multi-phase converter be controlled to deliver about the same current at any load level. Intersil multi-phase controllers guarantee current balance by comparing each channel's current to the average current delivered by all channels and making an appropriate adjustment to each channel's pulse width based on the error. Intersil's patented current-balance method is illustrated in Figure 5 where the average of the 2 or 3 sampled channel currents combines with the channel 1 sample,  $I_1$ , to create an error signal  $I_{ER}$ . The filtered error signal modifies the pulse width commanded by  $V_{COMP}$  to correct any unbalance and force  $I_{ER}$  toward zero.

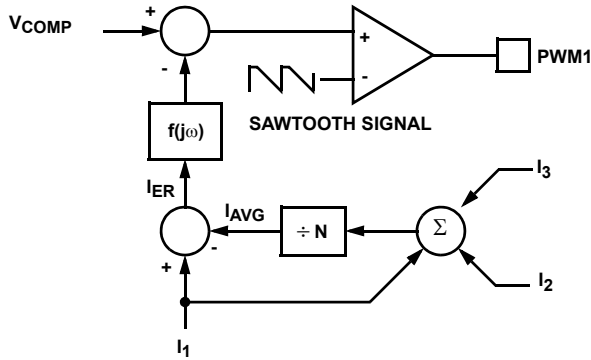


FIGURE 5. CHANNEL-1 PWM FUNCTION AND CURRENT-BALANCE ADJUSTMENT

In some circumstances, it may be necessary to deliberately design some channel-current unbalance into the system. In a highly compact design, one or two channels may be able to cool more effectively than the other(s) due to nearby air flow or heat sinking components. The other channel(s) may have more difficulty cooling with comparatively less air flow and heat sinking. The hotter channels may also be located close to other heat-generating components tending to drive their temperature even higher. In these cases, a proper selection of the current sense resistors ( $R_{ISEN}$  in Figure 4) introduces channel current unbalance into the system. Increasing the value of  $R_{ISEN}$  in the cooler channels and decreasing it in the hotter channels moves all channels into thermal balance at the expense of current balance.

**OVERCURRENT PROTECTION**

The average current,  $I_{AVG}$  in Figure 5, is continually compared with a constant  $75\mu A$  reference current. If the average current at any time exceeds the reference current, the comparator triggers the converter to shut down. All PWM signals are placed in a high-impedance state which signals the drivers to turn off both upper and lower MOSFETs. The system remains in this state while the controller counts 2048 phase-clock cycles.

This is followed by a soft-start attempt (see *Soft-Start*). If the soft-start attempt is successful, operation will continue as normal. Should the soft-start attempt fail, the ISL6219A repeats the 2048-cycle wait period and follows with another soft-start attempt. This hiccup mode of operation continues indefinitely as shown in Figure 6 as long as the controller is enabled or until the overcurrent condition resolves.

**VOLTAGE REGULATION**

The ISL6219A uses a digital to analog converter (DAC) to generate a reference voltage based on the logic signals at pins VID4 to VID0. The DAC decodes the a 5-bit logic signal (VID) into one of the discrete voltages shown in Table 1. Each VID input offers a 20mA pull up to 2.5V for use with open-drain outputs. External pull-up resistors or active-high outputstages can augment the pull-up current sources, but a slight accuracy error can occur if they are pulled above 2.9V.

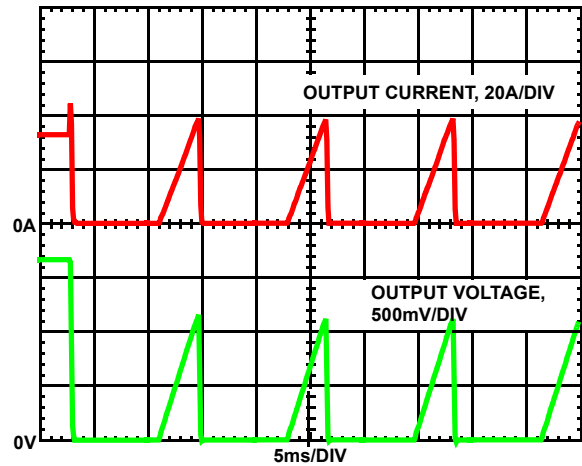


FIGURE 6. OVERCURRENT BEHAVIOR IN HICCUP MODE

The integrating compensation network shown in Figure 7 assures that the steady-state error in the output voltage is limited to the error in the reference voltage (output of the DAC) plus offset errors in the error amplifier. Intersil specifies the guaranteed tolerance of the ISL6219A to include all variations in the amplifiers and reference so that the output voltage remains within the specified system tolerance.

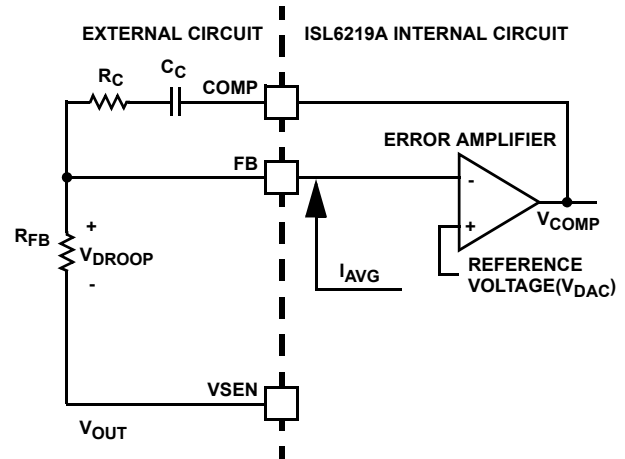


FIGURE 7. OUTPUT-VOLTAGE AND LOAD-LINE REGULATION



TABLE 1. VOLTAGE IDENTIFICATION CODES

VID4	VID3	VID2	VID1	VID0	VDAC
1	1	1	1	1	Off
1	1	1	1	0	1.100
1	1	1	0	1	1.125
1	1	1	0	0	1.150
1	1	0	1	1	1.175
1	1	0	1	0	1.200
1	1	0	0	1	1.225
1	1	0	0	0	1.250
1	0	1	1	1	1.275
1	0	1	1	0	1.300
1	0	1	0	1	1.325
1	0	1	0	0	1.350
1	0	0	1	1	1.375
1	0	0	1	0	1.400
1	0	0	0	1	1.425
1	0	0	0	0	1.450
0	1	1	1	1	1.475
0	1	1	1	0	1.500
0	1	1	0	1	1.525
0	1	1	0	0	1.550
0	1	0	1	1	1.575
0	1	0	1	0	1.600
0	1	0	0	1	1.625
0	1	0	0	0	1.650
0	0	1	1	1	1.675
0	0	1	1	0	1.700
0	0	1	0	1	1.725
0	0	1	0	0	1.750
0	0	0	1	1	1.775
0	0	0	1	0	1.800
0	0	0	0	1	1.825
0	0	0	0	0	1.850

### OVERVOLTAGE PROTECTION

If the ISL6219A detects output voltages above 115% of VID, the controller will immediately commands all PWM outputs low. This directs the Intersil drivers to turn on the lower MOSFETs and protect the load by preventing any further increase in output voltage. Once the output voltage falls to the level set by the VID code, the PWM outputs enter high-impedance mode. The Intersil drivers respond by turning off both upper and lower MOSFETs. If the overvoltage condition reoccurs, the ISL6219A will again command the lower MOSFETs to turn on. The

ISL6219A will continue to protect the load in this fashion as long as the overvoltage repeats.

After detecting an overvoltage condition, the ISL6219A terminates normal PWM operation until it is reset by one of two methods. Either by pulling VCC below the POR falling threshold and restoring it above the POR rising threshold or cycling FS/EN.

### Under-Voltage

The VSEN pin also detects when the CORE voltage drops below the VID programmed under-voltage falling threshold. This causes PGOOD to go low, but has no other effect on operation and is not latched.

### LOAD-LINE REGULATION

In applications with high transient current slew rates, the lowest-cost solution for maintaining regulation often requires some kind of controlled output impedance. A current proportional to the average current of all active channels is steered into the inverting input of the error amplifier. There is no DC return path connected to the FB pin except for the feedback resistor,  $R_{FB}$ . Therefore, the average current,  $I_{AVG}$ , produces a voltage drop across the feedback resistor,  $R_{FB}$ , proportional to the output current. In Figure 7, the steady-state value of  $V_{DROOP}$  is simply

$$V_{DROOP} = I_{AVG} R_{FB} \quad (\text{EQ. 3})$$

In the case that each channel uses the same value for  $R_{ISEN}$  to sense channel current, a more complete expression for  $V_{DROOP}$  can be determined from the expression for  $I_{AVG}$  as it is derived from Figures 4 and 5.

$$I_{AVG} = \frac{I_{OUT}}{N} \frac{r_{DS(ON)}}{R_{ISEN}}$$

$$V_{DROOP} = \frac{I_{OUT}}{N} \frac{r_{DS(ON)}}{R_{ISEN}} R_{FB} \quad (\text{EQ. 4})$$

### ENABLE AND DISABLE

Three separate input conditions must be met before the ISL6219A is released from shut-down mode. The PWM outputs are held in a high-impedance state to assure the drivers remain off during shut-down.

The internal power-on reset circuit (POR) prevents the ISL6219A from starting before the bias voltage at VCC reaches the POR-rising threshold as defined in *Electrical Specifications*. The rising threshold is high enough to guarantee that all parts of the ISL6219A can perform their functions properly. There is enough hysteresis in the POR-falling threshold to prevent nuisance tripping.

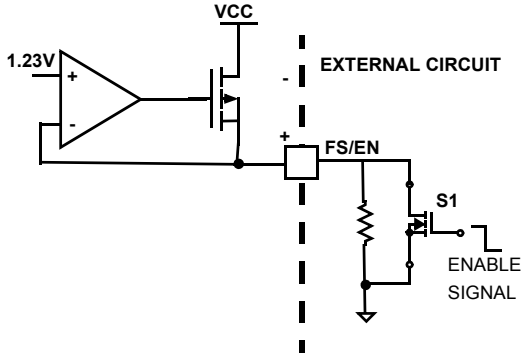


FIGURE 8. EXTERNAL ENABLE SIGNAL CIRCUIT

The frequency select/enable input (FS/EN) has a 1V threshold which must be exceeded before the internal oscillator begins running. An external enable signal should be used to control the gate of an external MOSFET tied to the FS/EN pin, see Figure 8. This MOSFET must pull FS/EN below the 1V threshold to disable the controller. When enabling the controller, this external enable circuit must release the FS/EN pin to float to the designed 1.23V level.

The 11111 VID code is reserved as a signal to the controller that no load is present. The controller will enter shut-down mode after receiving this code and will start up upon receiving any other code.

To enable the controller, VCC must be greater than the POR threshold; FS/EN must be greater than 1V; and VID cannot be equal to 11111. Once these conditions are true, the controller immediately initiates a soft start sequence.

### SOFT-START

After the POR function is completed with V<sub>CC</sub> reaching 4.38V, the soft-start sequence is initiated. Soft-Start, by its slow rise of CORE voltage from zero, avoids an over-current condition by slowly charging the output capacitors. This voltage rise is initiated by an internal DAC that slowly raises the reference voltage to the error amplifier input. The voltage rise is controlled by the oscillator frequency and the DAC within the controller, therefore, the output voltage is effectively regulated as it rises to the final programmed CORE voltage value.

For the first 32 PWM switching cycles, the DAC output remains inhibited and the PWM outputs remain in a high-impedance state. From the 33rd cycle and for another, approximately 150 cycles the PWM output remains low, clamping the lower output MOSFETs to ground. The time variability is due to the error amplifier, sawtooth generator and comparators moving into their active regions. After this short interval, the PWM outputs are enabled and increment the PWM pulse width from zero duty cycle to operational pulse width, thus allowing the output voltage to slowly reach the CORE voltage. The CORE voltage will reach its programmed value before the 2048 cycles, but the PGOOD output will not be initiated until the 2048th PWM switching cycle.

The soft-start time, t<sub>SS</sub>, is determined by an 11-bit counter that increments with every pulse of the phase clock. For example, a converter switching at 300kHz has a soft-start time of :

$$T_{SS} = \frac{2^{11}}{f_{SW}} = \frac{2048}{300\text{kHz}} = 6.8\text{ms} \quad (\text{EQ. 5})$$

Figure 9 shows the waveforms when the regulator is operating at 300kHz. Note that the soft-start duration is a function of the Channel Frequency as explained previously.

### DYNAMIC VID

The ISL6219A is capable of executing on-the-fly output-voltage changes. At the beginning of the phase-1 switching cycle (defined in the section entitled *PWM Operation*), the ISL6219A checks for a change in the VID code. The VID code is the bit pattern present at pins VID4-VID0 as outlined in *Voltage Regulation*. If the new code remains stable for another full cycle, the ISL6219A begins incrementing the reference by making 25mV change every two switching cycles until it reaches the new VID code.

Since the ISL6219A recognizes VID-code changes only at the beginning of a switching cycle, up to one full cycle may pass before a VID change registers. This is followed by a one-cycle wait before the output voltage begins to change. Thus, the total time required for a VID change, t<sub>DV</sub>, is dependent on the switching frequency (f<sub>S</sub>), the size of the change (ΔV<sub>ID</sub>), and the time before the next switching cycle begins. The one-cycle uncertainty in Equation 6 is due to the possibility that the VID code change may occur up to one full cycle before being recognized. The time required for a converter running with f<sub>S</sub> = 500kHz to make a 1.5V to 1.7V reference-voltage change is between 30μs and 32μs as calculated using Equation 6. This example is also illustrated in Figure 10.

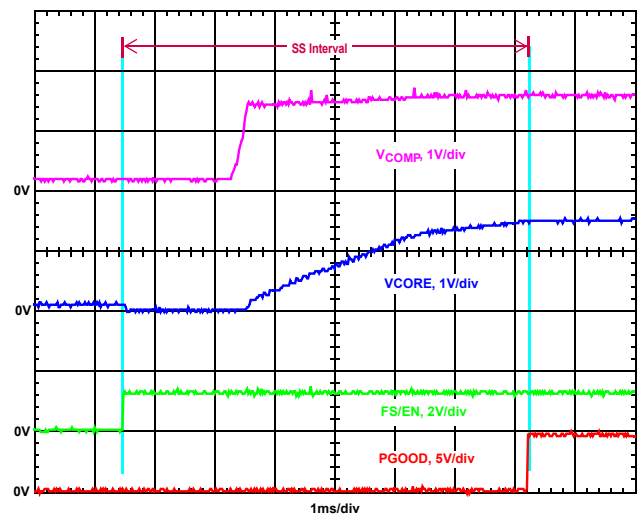
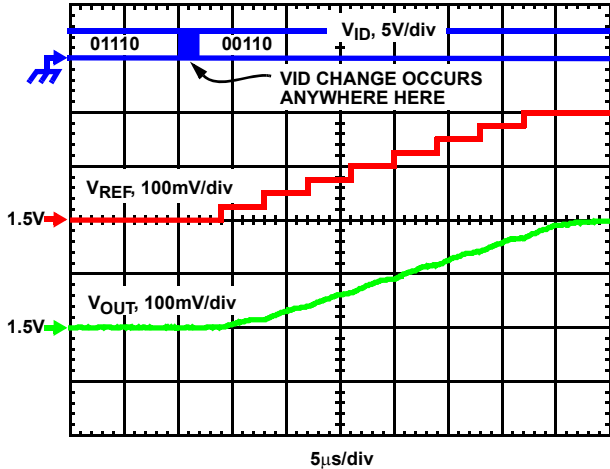


FIGURE 9. START-UP OF 3 PHASE SYSTEM OPERATING AT 300kHz



**FIGURE 10. DYNAMIC-VID WAVEFORMS FOR 500KHz ISL6219A BASED MULTI-PHASE BUCK CONVERTER**

$$\frac{1}{f_S} \left( \frac{2\Delta V_{ID}}{0.025} - 1 \right) < t_{DV} \leq \frac{1}{f_S} \left( \frac{2\Delta V_{ID}}{0.025} \right) \quad (\text{EQ. 6})$$

### General Design Guide

This design guide is intended to provide a high-level explanation of the steps necessary to create a multi-phase power converter. It is assumed that the reader is familiar with many of the basic skills and techniques referenced below. In addition to this guide, Intersil provides complete reference designs that include schematics, bills of materials, and example board layouts for all common microprocessor applications.

### Power Stages

The first step in designing a multi-phase converter is to determine the number of phases. This determination depends heavily on the cost analysis which in turn depends on system constraints that differ from one design to the next. Principally, the designer will be concerned with whether components can be mounted on both sides of the circuit board; whether through-hole components are permitted on either side; and the total board space available for power-supply circuitry. Generally speaking, the most economical solutions will be for each phase to handle between 15 and 20A. All-surface-mount designs will tend toward the lower end of this current range and, if through-hole MOSFETs can be used, higher per-phase currents are possible. In cases where board space is the limiting constraint, current can be pushed as high as 30A per phase, but these designs require heat sinks and forced air to cool the MOSFETs.

### MOSFETs

The choice of MOSFETs depends on the current each MOSFET will be required to conduct; the switching frequency; the capability of the MOSFETs to dissipate heat; and the availability and nature of heat sinking and air flow.

### LOWER MOSFET POWER CALCULATION

The calculation for heat dissipated in the lower MOSFET is simple, since virtually all of the heat loss in the lower MOSFET is due to current conducted through the channel resistance ( $r_{DS(ON)}$ ). In Equation 7,  $I_M$  is the maximum continuous output current;  $I_{L,PP}$  is the peak-to-peak inductor current (see Equation 1);  $d$  is the duty cycle ( $V_{OUT}/V_{IN}$ ); and  $L$  is the per-channel inductance.

$$P_{LOW,1} = r_{DS(ON)} \left[ \left( \frac{I_M}{N} \right)^2 (1-d) + \frac{I_{L,PP}^2 (1-d)}{12} \right] \quad (\text{EQ. 7})$$

An additional term can be added to the lower-MOSFET loss equation to account for additional loss accrued during the dead time when inductor current is flowing through the lower-MOSFET body diode. This term is dependent on the diode forward voltage at  $I_M$ ,  $V_{D(ON)}$ ; the switching frequency,  $f_S$ ; and the length of dead times,  $t_{d1}$  and  $t_{d2}$ , at the beginning and the end of the lower-MOSFET conduction interval respectively.

$$P_{LOW,2} = V_{D(ON)} f_S \left[ \left( \frac{I_M}{N} + \frac{I_{PP}}{2} \right) t_{d1} + \left( \frac{I_M}{N} - \frac{I_{PP}}{2} \right) t_{d2} \right] \quad (\text{EQ. 8})$$

Thus the total power dissipated in each lower MOSFET is approximated by the summation of  $P_L$  and  $P_D$ .

### UPPER MOSFET POWER CALCULATION

In addition to  $r_{DS(ON)}$  losses, a large portion of the upper-MOSFET losses are due to currents conducted across the input voltage ( $V_{IN}$ ) during switching. Since a substantially higher portion of the upper-MOSFET losses are dependant on switching frequency, the power calculation is somewhat more complex. Upper MOSFET losses can be divided into separate components involving the upper-MOSFET switching times; the lower-MOSFET body-diode reverse-recovery charge,  $Q_{rr}$ ; and the upper MOSFET  $r_{DS(ON)}$  conduction loss.

When the upper MOSFET turns off, the lower MOSFET does not conduct any portion of the inductor current until the voltage at the phase node falls below ground. Once the lower MOSFET begins conducting, the current in the upper MOSFET falls to zero as the current in the lower MOSFET ramps up to assume the full inductor current. In Equation 9, the required time for this commutation is  $t_1$  and the associated power loss is  $P_{UP,1}$ .

$$P_{UP,1} \approx V_{IN} \left( \frac{I_M}{N} + \frac{I_{L,PP}}{2} \right) \left( \frac{t_1}{2} \right) f_S \quad (\text{EQ. 9})$$

Similarly, the upper MOSFET begins conducting as soon as it begins turning on. In Equation 10, this transition occurs over a time  $t_2$ , and the approximate the power loss is  $P_{UP,2}$ .

$$P_{UP,2} \approx V_{IN} \left( \frac{I_M}{N} - \frac{I_{L,PP}}{2} \right) \left( \frac{t_2}{2} \right) f_S \quad (\text{EQ. 10})$$

A third component involves the lower MOSFET's reverse-recovery charge,  $Q_{rr}$ . Since the inductor current has fully commutated to the upper MOSFET before the lower-MOSFET's body diode can recover all of  $Q_{rr}$ , it is conducted through the upper MOSFET across  $V_{IN}$ . The power dissipated as a result is  $P_{UP,3}$  and is simply:

$$P_{UP,3} = V_{IN} Q_{rr} f_S \quad (\text{EQ. 11})$$

Finally, the resistive part of the upper MOSFET's is given in Equation 12 as  $P_{UP,4}$ .

$$P_{UP,4} = r_{DS(ON)} \left[ \left( \frac{I_M}{N} \right)^2 d + \frac{I_{PP}^2}{12} \right] \quad (\text{EQ. 12})$$

In this case, of course,  $r_{DS(ON)}$  is the on resistance of the upper MOSFET.

The total power dissipated by the upper MOSFET at full load can now be approximated as the summation of the results from Equations 9, 10, 11 and 12. Since the power equations depend on MOSFET parameters, choosing the correct MOSFETs can be an iterative process that involves repetitively solving the loss equations for different MOSFETs and different switching frequencies until converging upon the best solution.

### Current Sensing

Pins 23, 20 and 19 are the ISEN pins denoted ISEN1, ISEN2 and ISEN3, respectively. The resistors connected between these pins and the phase nodes determine the gains in the load-line regulation loop and the channel-current balance loop. Select the values for these resistors based on the room temperature  $r_{DS(ON)}$  of the lower MOSFETs; the full-load operating current,  $I_{FL}$ ; and the number of phases,  $N$  according to Equation 13 (see also Figure 4).

$$R_{ISEN} = \frac{r_{DS(ON)} I_{FL}}{50 \times 10^{-6} N} \quad (\text{EQ. 13})$$

In certain circumstances, it may be necessary to adjust the value of one or more of the ISEN resistors. This can arise when the components of one or more channels are inhibited from dissipating their heat so that the affected channels run hotter than desired (see the section entitled *Channel-Current Balance*). In these cases, choose new, smaller values of  $R_{ISEN}$  for the affected phases. Choose  $R_{ISEN,2}$  in proportion to the desired decrease in temperature rise in order to cause proportionally less current to flow in the hotter phase.

$$R_{ISEN,2} = R_{ISEN} \frac{\Delta T_2}{\Delta T_1} \quad (\text{EQ. 14})$$

In Equation 14, make sure that  $\Delta T_2$  is the desired temperature rise above the ambient temperature, and  $\Delta T_1$  is the measured temperature rise above the ambient temperature. While a single adjustment according to Equation 14 is usually sufficient, it may occasionally be necessary to adjust  $R_{ISEN}$  two or more times to achieve perfect thermal balance between all channels.

### Load-Line Regulation Resistor

The load-line regulation resistor is labeled  $R_{FB}$  in Figure 7. Its value depends on the desired full-load droop voltage ( $V_{DROOP}$  in Figure 7). If Equation 13 is used to select each ISEN resistor, the load-line regulation resistor is as shown in Equation 15.

$$R_{FB} = \frac{V_{DROOP}}{50 \times 10^{-6}} \quad (\text{EQ. 15})$$

If one or more of the ISEN resistors was adjusted for thermal balance as in Equation 14, the load-line regulation resistor should be selected according to Equation 16 where  $I_{FL}$  is the full-load operating current and  $R_{ISEN(n)}$  is the ISEN resistor connected to the  $n^{\text{th}}$  ISEN pin.

$$R_{FB} = \frac{V_{DROOP}}{I_{FL} r_{DS(ON)}} \sum_n R_{ISEN(n)} \quad (\text{EQ. 16})$$

### Compensation

The two opposing goals of compensating the voltage regulator are stability and speed. Depending on whether the regulator employs the optional load-line regulation as described in *Load-Line Regulation*, there are two distinct methods for achieving these goals.

### COMPENSATING A LOAD-LINE REGULATED CONVERTER

The load-line regulated converter behaves in a similar manner to a peak-current mode controller because the two poles at the output-filter L-C resonant frequency split with the introduction of current information into the control loop. The final location of

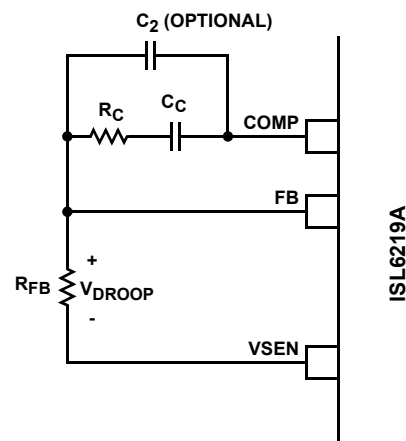


FIGURE 11. COMPENSATION CONFIGURATION FOR LOAD-LINE REGULATED ISL6219A CIRCUIT

these poles is determined by the system function, the gain of the current signal, and the value of the compensation components,  $R_C$  and  $C_C$ .

Since the system poles and zero are effected by the values of the components that are meant to compensate them, the solution to the system equation becomes fairly complicated. Fortunately there is a simple approximation that comes very close to an optimal solution. Treating the system as though it were a voltage-mode regulator by compensating the L-C poles and the ESR zero of the voltage-mode approximation yields a solution that is always stable with very close to ideal transient performance.

The feedback resistor,  $R_{FB}$ , has already been chosen as outlined in *Load-Line Regulation Resistor*. Select a target bandwidth for the compensated system,  $f_0$ . The target bandwidth must be large enough to assure adequate transient performance, but smaller than 1/3 of the per-channel switching frequency. The values of the compensation components depend on the relationships of  $f_0$  to the L-C pole frequency and the ESR zero frequency. For each of the three cases defined in the following, there is a separate set of equations for the compensation components

$$\text{Case 1: } \frac{1}{2\pi\sqrt{LC}} > f_0$$

$$R_C = R_{FB} \frac{2\pi f_0 V_{PP} \sqrt{LC}}{0.75 V_{IN}}$$

$$C_C = \frac{0.75 V_{IN}}{2\pi V_{PP} R_{FB} f_0}$$

$$\text{Case 2: } \frac{1}{2\pi\sqrt{LC}} \leq f_0 < \frac{1}{2\pi C(\text{ESR})}$$

$$R_C = R_{FB} \frac{V_{PP}(2\pi)^2 f_0^2 LC}{0.75 V_{IN}} \quad (\text{EQ. 17})$$

$$C_C = \frac{0.75 V_{IN}}{(2\pi)^2 f_0^2 V_{PP} R_{FB} \sqrt{LC}}$$

$$\text{Case 3: } f_0 > \frac{1}{2\pi C(\text{ESR})}$$

$$R_C = R_{FB} \frac{2\pi f_0 V_{PP} L}{0.75 V_{IN}(\text{ESR})}$$

$$C_C = \frac{0.75 V_{IN}(\text{ESR}) \sqrt{C}}{2\pi V_{PP} R_{FB} f_0 \sqrt{L}}$$

In Equations *17*,  $L$  is the per-channel filter inductance divided by the number of active channels;  $C$  is the sum total of all output capacitors;  $\text{ESR}$  is the equivalent-series resistance of the bulk output-filter capacitance; and  $V_{PP}$  is the peak-to-peak sawtooth signal amplitude as described in Figure 5 and *Electrical Specifications* on page 4.

Once selected, the compensation values in Equations 17 assure a stable converter with reasonable transient performance. In most cases, transient performance can be improved by making adjustments to  $R_C$ . Slowly increase the value of  $R_C$

while observing the transient performance on an oscilloscope until no further improvement is noted. Normally,  $C_C$  will not need adjustment. Keep the value of  $C_C$  from Equations 17 unless some performance issue is noted.

The optional capacitor  $C_2$ , is sometimes needed to bypass noise away from the PWM comparator (see Figure 5). Keep a position available for  $C_2$ , and be prepared to install a high-frequency capacitor of between 22pF and 150pF in case any jitter problem is noted.

### COMPENSATION WITHOUT LOAD-LINE REGULATION

The non load-line regulated converter is accurately modeled as a voltage-mode regulator with two poles at the L-C resonant frequency and a zero at the ESR frequency. A type III controller, as shown in Figure 12, provides the necessary compensation.

The first step is to choose the desired bandwidth,  $f_0$ , of the compensated system. Choose a frequency high enough to assure adequate transient performance but not higher than 1/3 of the switching frequency. The type-III compensator has an extra high-frequency pole,  $f_{HF}$ . This pole can be used for added noise rejection or to assure adequate attenuation at the error-amplifier high-order pole and zero frequencies. A good general rule is to chose  $f_{HF} = 10 f_0$ , but it can be higher if desired. Choosing  $f_{HF}$  to be lower than  $10 f_0$  can cause problems with too much phase shift below the system bandwidth.

In the solutions to the compensation equations, there is a single degree of freedom. For the solutions presented in Equations 18,  $R_{FB}$  is selected arbitrarily. The remaining compensation components are then selected according to Equation 18.

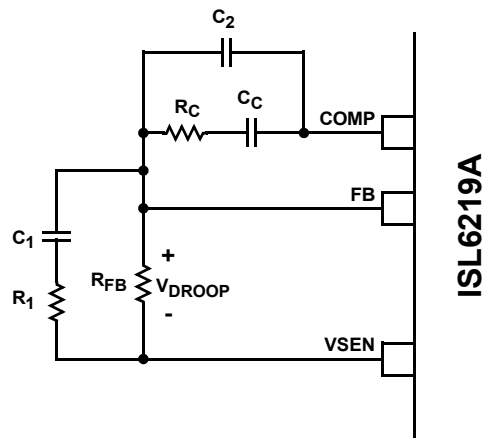


FIGURE 12. COMPENSATION CIRCUIT FOR ISL6219A BASED CONVERTER WITHOUT LOAD-LINE REGULATION.

$$\begin{aligned}
 C_1 &= \frac{\sqrt{LC} - C(\text{ESR})}{R_{\text{FB}}} \\
 R_C &= \frac{V_{\text{PP}}(2\pi)^2 f_0 f_{\text{HF}} LC}{0.75 V_{\text{IN}} \left[ 2\pi f_{\text{HF}} (\sqrt{LC} - 1) \right]} \\
 R_1 &= R_{\text{FB}} \frac{C(\text{ESR})}{\sqrt{LC} - C(\text{ESR})} \\
 C_2 &= \frac{0.75 V_{\text{IN}}}{(2\pi)^2 f_0 f_{\text{HF}} \sqrt{LC} R_{\text{FB}} V_{\text{PP}}} \\
 C_C &= \frac{0.75 V_{\text{IN}}}{2\pi V_{\text{PP}} R_{\text{FB}} f_0 \left( 1 - \frac{1}{2\pi f_{\text{HF}} \sqrt{LC}} \right)} \quad (\text{EQ. 18})
 \end{aligned}$$

In Equation 18,  $L$  is the per-channel filter inductance divided by the number of active channels;  $C$  is the sum total of all output capacitors;  $\text{ESR}$  is the equivalent-series resistance of the bulk output-filter capacitance; and  $V_{\text{PP}}$  is the peak-to-peak sawtooth signal amplitude as described in Figure 5 and *Electrical Specifications* on page 4.

## OUTPUT FILTER DESIGN

The output inductors and the output capacitor bank together form a low-pass filter responsible for smoothing the pulsating voltage at the phase nodes. The output filter also must provide the transient energy during the interval of time after the beginning of the transient until the regulator can fully respond. Because it has a low bandwidth compared to the switching frequency, the output filter necessarily limits the system transient response leaving the output capacitor bank to supply or sink load current while the current in the output inductors increases or decreases to meet the demand.

In high-speed converters, the output capacitor bank is usually the most costly (and often the largest) part of the circuit. Output filter design begins with minimizing the cost of this part of the circuit. The critical load parameters in choosing the output capacitors are the maximum size of the load step,  $\Delta I$ ; the load-current slew rate,  $di/dt$ ; and the maximum allowable output-voltage deviation under transient loading,  $\Delta V_{\text{MAX}}$ . Capacitors are characterized according to their capacitance,  $\text{ESR}$ , and  $\text{ESL}$  (equivalent series inductance).

At the beginning of the load transient, the output capacitors supply all of the transient current. The output voltage will initially deviate by an amount approximated by the voltage drop across the  $\text{ESL}$ . As the load current increases, the voltage drop across the  $\text{ESR}$  increases linearly until the load current reaches its final value. The capacitors selected must have sufficiently low  $\text{ESL}$  and  $\text{ESR}$  so that the total output voltage deviation is less than the allowable maximum. Neglecting the

contribution of inductor current and regulator response, the output voltage initially deviates by an amount:

$$\Delta V \approx (\text{ESL}) \frac{di}{dt} + (\text{ESR}) \Delta I \quad (\text{EQ. 19})$$

The filter capacitor must have sufficiently low  $\text{ESL}$  and  $\text{ESR}$  so that  $\Delta V < \Delta V_{\text{MAX}}$ .

Most capacitor solutions rely on a mixture of high-frequency capacitors with relatively low capacitance in combination with bulk capacitors having high capacitance but limited high-frequency performance. Minimizing the  $\text{ESL}$  of the high-frequency capacitors allows them to support the output voltage as the current increases. Minimizing the  $\text{ESR}$  of the bulk capacitors allows them to supply the increased current with less output voltage deviation.

The  $\text{ESR}$  of the bulk capacitors also creates the majority of the output-voltage ripple. As the bulk capacitors sink and source the inductor ac ripple current (see *Interleaving* and Equation 2), a voltage develops across the bulk-capacitor  $\text{ESR}$  equal to  $I_{\text{PP}}(\text{ESR})$ . Thus, once the output capacitors are selected, the maximum allowable ripple voltage,  $V_{\text{PP}}(\text{MAX})$ , determines the a lower limit on the inductance.

$$L \geq (\text{ESR}) \frac{(V_{\text{IN}} - NV_{\text{OUT}}) V_{\text{OUT}}}{f_s V_{\text{IN}} V_{\text{PP}}(\text{MAX})} \quad (\text{EQ. 20})$$

Since the capacitors are supplying a decreasing portion of the load current while the regulator recovers from the transient, the capacitor voltage becomes slightly depleted. The output inductors must be capable of assuming the entire load current before the output voltage decreases more than  $\Delta V_{\text{MAX}}$ . This places an upper limits on inductance.

$$L \leq \frac{2NCV_O}{(\Delta I)^2} [\Delta V_{\text{MAX}} - \Delta I(\text{ESR})] \quad (\text{EQ. 21})$$

$$L \leq \frac{(1.25)NC}{(\Delta I)^2} [\Delta V_{\text{MAX}} - \Delta I(\text{ESR})] (V_{\text{IN}} - V_O) \quad (\text{EQ. 22})$$

Equation 22 gives the upper limit on  $L$  for the cases when the trailing edge of the current transient causes a greater output-voltage deviation than the leading edge. Equation 21 addresses the leading edge. Normally, the trailing edge dictates the selection of  $L$  because duty cycles are usually less than 50%.

Nevertheless, both inequalities should be evaluated, and  $L$  should be selected based on the lower of the two results. In each equation,  $L$  is the per-channel inductance,  $C$  is the total output capacitance, and  $N$  is the number of active channels.

**Switching Frequency**

There are a number of variables to consider when choosing the switching frequency. There are considerable effects on the upper-MOSFET loss calculation and, to a lesser extent, the lower-MOSFET loss calculation. These effects are outlined in *MOSFETs*, and they establish the upper limit for the switching frequency. The lower limit is established by the requirement for fast transient response and small output-voltage ripple as outlined in *Output Filter Design*. Choose the lowest switching frequency that allows the regulator to meet the transient-response requirements. Switching frequency is determined by the selection of the frequency-setting resistor,  $R_T$  (see the figure *Typical Application* on page 3). Figure 13 and Equation 23 are provided to assist in the selecting the correct value for  $R_T$ .

$$R_T = 10^{[11.09 - 1.13 \log(f_s)]} \quad (\text{EQ. 23})$$

Figures 14 and 15 can be used to determine the input-capacitor rms current as of duty cycle, maximum sustained output current ( $I_O$ ), and the ratio of the combined peak-to-peak inductor current ( $I_{L,PP}$ ) to  $I_O$ . Figure 16 is provided as a reference to demonstrate the dramatic reductions in input-capacitor rms current upon the implementation of the multiphase topology.

**Input Capacitor Selection**

The input capacitors are responsible for sourcing the ac component of the input current flowing into the upper MOSFETs. Their rms current capacity must be sufficient to handle the ac component of the current drawn by the upper MOSFETs which is related to duty cycle and the number of active phases.

Figures 14 and 15 can be used to determine the input-capacitor RMS current as of duty cycle, maximum sustained output current ( $I_O$ ), and the ratio of the combined peak-to-peak inductor current ( $I_{L,PP}$ ) to  $I_O$ . Figure 16 is provided as a reference to demonstrate the dramatic reductions in input-capacitor rms current upon the implementation of the multiphase topology.

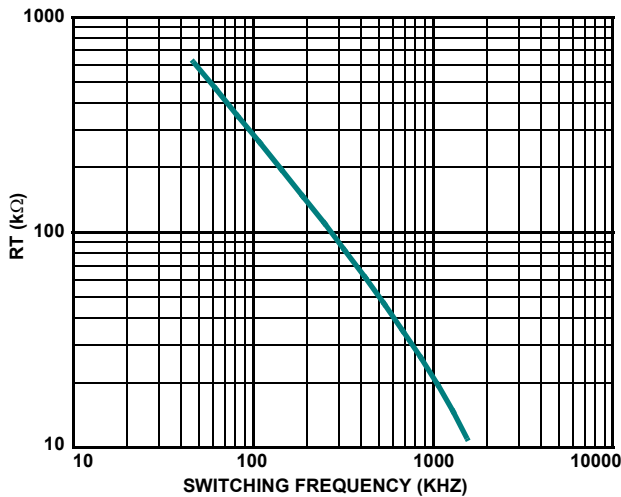


FIGURE 13.  $R_T$  VS SWITCHING FREQUENCY

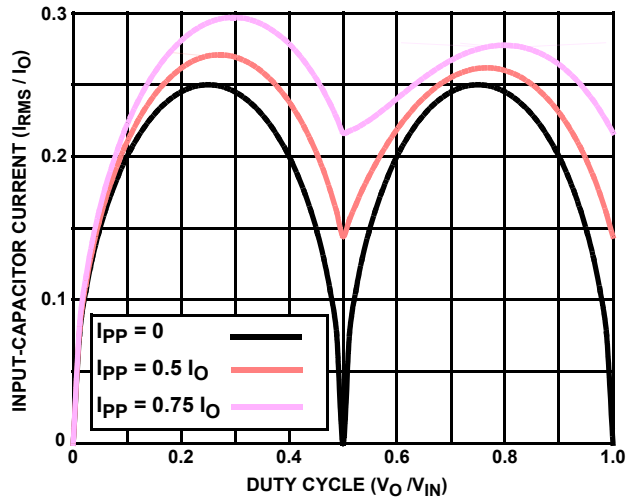


FIGURE 14. NORMALIZED INPUT-CAPACITOR RMS CURRENT VS DUTY CYCLE FOR 2-PHASE CONVERTER

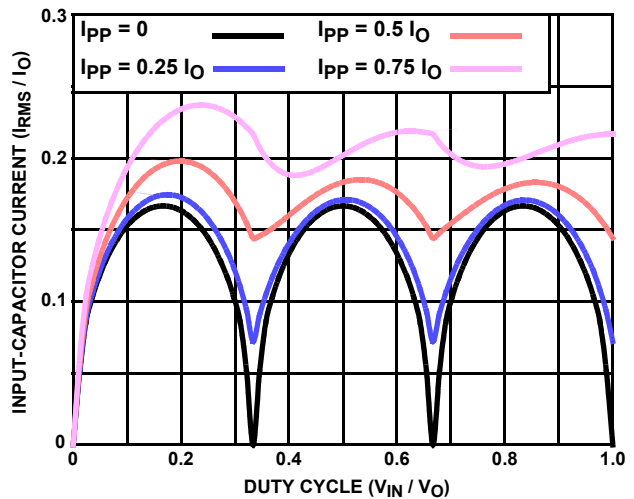


FIGURE 15. NORMALIZED INPUT-CAPACITOR RMS CURRENT VS DUTY CYCLE FOR 3-PHASE

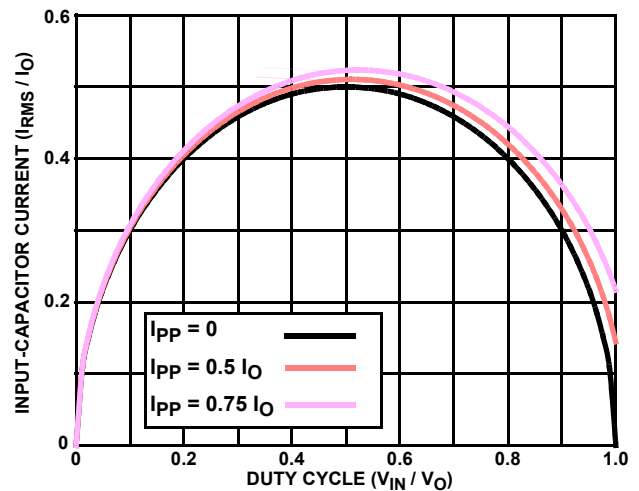
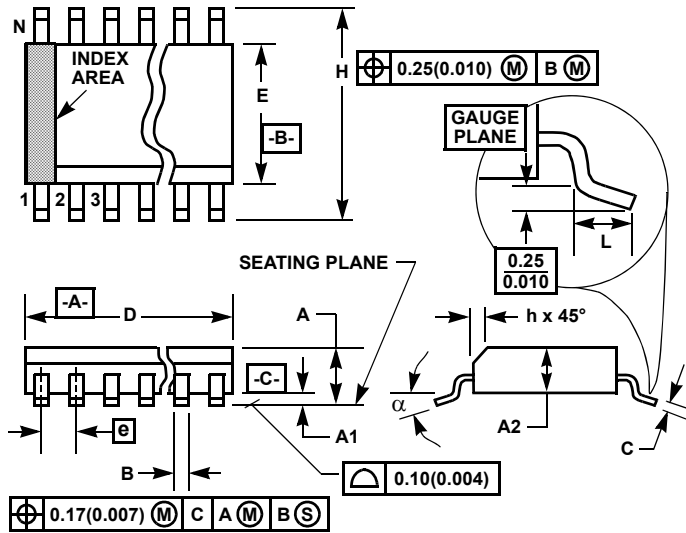


FIGURE 16. NORMALIZED INPUT-CAPACITOR RMS CURRENT VS DUTY CYCLE FOR SINGLE-PHASE CONVERTER

**Shrink Small Outline Plastic Packages (SSOP)  
Quarter Size Outline Plastic Packages (QSOP)**



**M28.15**

**28 LEAD SHRINK SMALL OUTLINE PLASTIC PACKAGE  
(0.150" WIDE BODY)**

SYMBOL	INCHES		MILLIMETERS		NOTES
	MIN	MAX	MIN	MAX	
A	0.053	0.069	1.35	1.75	-
A1	0.004	0.010	0.10	0.25	-
A2	-	0.061	-	1.54	-
B	0.008	0.012	0.20	0.30	9
C	0.007	0.010	0.18	0.25	-
D	0.386	0.394	9.81	10.00	3
E	0.150	0.157	3.81	3.98	4
e	0.025 BSC		0.635 BSC		-
H	0.228	0.244	5.80	6.19	-
h	0.0099	0.0196	0.26	0.49	5
L	0.016	0.050	0.41	1.27	6
N	28		28		7
$\alpha$	0°	8°	0°	8°	-

Rev. 1 6/04

**NOTES:**

1. Symbols are defined in the "MO Series Symbol List" in Section 2.2 of Publication Number 95.
2. Dimensioning and tolerancing per ANSI Y14.5M-1982.
3. Dimension "D" does not include mold flash, protrusions or gate burrs. Mold flash, protrusion and gate burrs shall not exceed 0.15mm (0.006 inch) per side.
4. Dimension "E" does not include interlead flash or protrusions. Interlead flash and protrusions shall not exceed 0.25mm (0.010 inch) per side.
5. The chamfer on the body is optional. If it is not present, a visual index feature must be located within the crosshatched area.
6. "L" is the length of terminal for soldering to a substrate.
7. "N" is the number of terminal positions.
8. Terminal numbers are shown for reference only.
9. Dimension "B" does not include dambar protrusion. Allowable dambar protrusion shall be 0.10mm (0.004 inch) total in excess of "B" dimension at maximum material condition.
10. Controlling dimension: INCHES. Converted millimeter dimensions are not necessarily exact.

© Copyright Intersil Americas LLC 2002-2007. All Rights Reserved.  
All trademarks and registered trademarks are the property of their respective owners.

For additional products, see [www.intersil.com/en/products.html](http://www.intersil.com/en/products.html)

Intersil products are manufactured, assembled and tested utilizing ISO9001 quality systems as noted in the quality certifications found at [www.intersil.com/en/support/qualandreliability.html](http://www.intersil.com/en/support/qualandreliability.html)

*Intersil products are sold by description only. Intersil may modify the circuit design and/or specifications of products at any time without notice, provided that such modification does not, in Intersil's sole judgment, affect the form, fit or function of the product. Accordingly, the reader is cautioned to verify that datasheets are current before placing orders. Information furnished by Intersil is believed to be accurate and reliable. However, no responsibility is assumed by Intersil or its subsidiaries for its use; nor for any infringements of patents or other rights of third parties which may result from its use. No license is granted by implication or otherwise under any patent or patent rights of Intersil or its subsidiaries.*

For information regarding Intersil Corporation and its products, see [www.intersil.com](http://www.intersil.com)